

RESEARCH ARTICLE

GENOMICS OF AGING

Origins and evolution of extreme life span in Pacific Ocean rockfishes

Sree Rohit Raj Kolora^{1†}, Gregory L. Owens^{1,2†}, Juan Manuel Vazquez¹, Alexander Stubbs¹, Kamalakar Chatla¹, Conner Jainese³, Katelyn Seeto³, Merit McCrea³, Michael W. Sandel⁴, Juliana A. Vianna⁵, Katherine Maslenikov⁶, Doris Bachtrog¹, James W. Orr⁶, Milton Love³, Peter H. Sudmant^{1,7*}

Pacific Ocean rockfishes (genus *Sebastodes*) exhibit extreme variation in life span, with some species being among the most long-lived extant vertebrates. We de novo assembled the genomes of 88 rockfish species and from these identified repeated signatures of positive selection in DNA repair pathways in long-lived taxa and 137 longevity-associated genes with direct effects on life span through insulin signaling and with pleiotropic effects through size and environmental adaptations. A genome-wide screen of structural variation reveals copy number expansions in the immune modulatory butyrophilin gene family in long-lived species. The evolution of different rockfish life histories is coupled to genetic diversity and reshapes the mutational spectrum driving segregating CpG→TpG variants in long-lived species. These analyses highlight the genetic innovations that underlie life history trait adaptations and, in turn, how they shape genomic diversity.

Decades of theoretical work on the evolution of aging have demonstrated that senescence is a “theoretically inevitable” consequence of the increased selective impact of genes that influence early-life survival and fecundity compared with genes that act late in life (1). Nonetheless, across vertebrates alone, life span varies by more than three orders of magnitude, ranging from the 5-week life cycle of the pygmy goby (2) to the ~400-year life span of the Greenland shark (3), highlighting exceptional diversity of this trait across species. Understanding evolutionary transitions in life span can highlight diverse genetic mechanisms of life-span control and the subsequent impacts of life-history shifts on patterns of genetic diversity.

Across organisms, aging is accompanied by several molecular hallmarks including genome instability, loss of protein homeostasis, and mitochondrial dysfunction, among others (4). Vertebrates in particular also exhibit a number of distinct hallmarks of aging that are directly linked to human disease and

health span, such as immunosenescence, inflammation, and stem cell exhaustion (5). Thus, understanding the underpinnings of life-span variation across vertebrate taxa can provide critical insights into the maintenance of human health and vigor in old age.

Rockfishes (genus *Sebastodes*) of the Pacific Ocean exhibit life spans ranging from 11 years (*Sebastodes minor*) to >200 years (rougheye rockfish, *Sebastodes aleutianus*) (6) (Fig. 1A). This phenotype exhibits a relatively uniform distribution across the more than 75 different species of this clade for which detailed longevity information is available (fig. S1). Rockfishes are thus distinctive in that while some species are among the longest-lived vertebrates known to exist, life span can widely range even among closely related taxa. More than 120 different species of rockfish are found throughout the northeast and northwest Pacific Ocean (7) (Fig. 1B). This abundance of species with vastly differing life histories represents an example of repeated, recent adaptations that have reshaped longevity phenotypes.

Results

Sequencing and assembly of 102 rockfish genomes

To dissect the genetic underpinnings of life-span variation and adaptation, we sequenced and de novo assembled the genomes of 102 rockfish individuals encompassing 88 different species, including 79 members of the *Sebastodes* clade and nine closely related outgroup taxa (figs. S1 and S2). Long-read Pacific Biosciences genome assemblies were generated for six *Sebastodes* species and the outgroup

Sebastolobus alascanus [mean contig N50: 6.1 million base pairs (Mbp)] (Fig. 1C). Five of these *Sebastodes* genomes were scaffolded with long-range Hi-C data, resulting in chromosome-scale assemblies (mean scaffold N50: 34.1 Mbp) (Fig. 1C, table S1, and fig. S3). High-coverage Illumina-based assemblies were generated for 71 additional *Sebastodes* species (mean contig N50: 73.8 kilobase pairs). Genome completeness [assessed by BUSCO scores (8)] ranged from an average of 97.9% for long-read-based genomes to 91.2% for Illumina-based assemblies, and the majority (five of seven) of the long-read-based genomes reached QV40 base quality (average QV39 for all seven) (fig. S4). Transcriptomes were generated from brain and eye tissue for eight species, including six individuals for which we generated long-read-based genome assemblies to assist in gene annotation. In total, we identified ~25,000 protein-coding genes on average across the seven long-read genome assemblies (table S3). Together, these genome assemblies encompass the majority of species represented in the *Sebastodes* genus and almost all representatives for which detailed life-span information has been cataloged, including a chromosome-level assembly of the ultra-long-lived *S. aleutianus*.

We established the phylogenetic relationships and speciation times among rockfish species by constructing an ultrametric species phylogeny [see supplementary methods (9)] (Fig. 1A). The topology of this tree is consistent with previous phylogenetic analyses of rockfishes (7, 10). The varied placement of long-lived taxa in the tree suggests repeated life span-related evolution (Fig. 1A), which is supported by character mapping analysis that shows multiple independent gains of long life span (fig. S7).

Repeated signatures of positive selection in DNA repair pathways in long-lived taxa

We next sought to determine the genetic underpinnings of life span in Pacific rockfishes. We used a branch-site model test of codon evolution to identify candidates of positive selection in the longest-lived (≥ 105 years) and shortest-lived (≤ 20 years) species (life span decile tails, $n = 7$ species), identifying 772 and 873 genes, respectively. Most of these positively selected genes (PSGs) were lineage specific, although ~12 to 15% of genes (127 and 118, respectively) were present in two or more species, representing either selection on the ancestral branch or convergent evolution. Additionally, 180 PSGs were found in both long- and short-lived individuals, highlighting that many of these genes may be under selection for other traits. Whereas no pathways were enriched in PSGs in short-lived species after multiple testing correction, PSGs in long-lived species were enriched for DNA double-stranded break repair pathways (Fig. 2A and table S5).

¹Department of Integrative Biology, University of California, Berkeley, CA, USA. ²Department of Biology, University of Victoria, Victoria, BC, Canada. ³Marine Sciences Institute, University of California, Santa Barbara, CA, USA.

⁴Department of Biological and Environmental Sciences, University of West Alabama, Livingston, AL, USA.

⁵Departamento de Ecosistemas y Medio Ambiente, Pontificia Universidad Católica de Chile, Santiago, Chile. ⁶School of Aquatic and Fishery Sciences and Burke Museum of Natural History and Culture, University of Washington, Seattle, WA, USA. ⁷Center for Computational Biology, University of California, Berkeley, CA, USA.

*Corresponding author. Email: psudmant@berkeley.edu

†These authors contributed equally to this work.

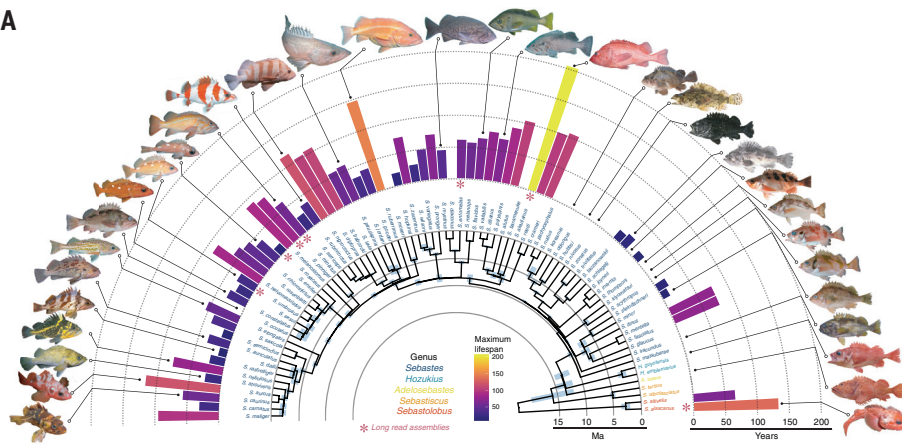
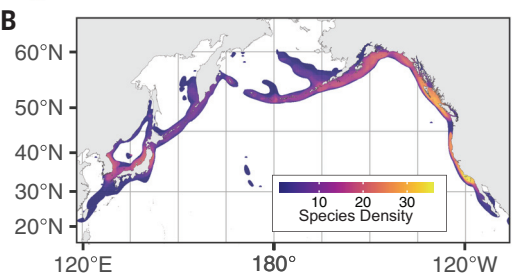
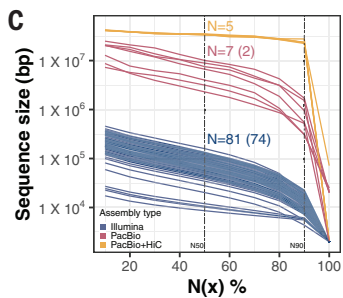
A**B****C**

Fig. 1. Genome assemblies and relationships among rockfish species. (A) Ultrametric tree of the rockfish species sequenced in this study and their associated maximum life spans along with representative images (node timing confidence intervals in light blue) created using IQ-TREE, ASTRAL (Accurate Species Tree Algorithm), and BPPR. Asterisks indicate individuals for which long-read sequencing-based genomes were assembled. (B) The density of rockfish species (heatmap colors) throughout the Pacific Ocean. (C) Genome assembly statistics for 81 species, blue and pink represent $N(x)$ contig lengths, while orange indicates $N(x)$ scaffold lengths.

The enrichment in DNA replication, repair, and maintenance is driven by 16 genes (Fig. 2B), five of which exhibit selective signatures in more than one species. These include genes in pathways associated with life span across organisms, such as telomere maintenance (e.g., *WRAP53* and *DCLRE1B*) and base excision repair (e.g., *FEN1*). Intriguingly, adaptive signatures in *DCLRE1B* and *FEN1* have been identified in the bowhead whale and giant tortoise, respectively (11, 12). MCM6, a core member of the DNA replication helicase machinery, exhibits signatures of positive selection in *S. ruberrimus* and *S. nigricinctus*. These signatures of selection suggest that repeated transitions in life span in rockfishes are likely enabled by parallel evolution of different genes in shared critical DNA maintenance pathways.

Genes associated with life-span adaptations through direct and pleiotropic effects

We next examined the role of evolution in convergent genes and pathways on rockfish life span by comparing the relative evolutionary rates of genes across the phylogeny (13). This approach allowed us to identify genes

with evolutionary rates that are correlated, either positively or negatively, with life span (Fig. 2C and table S14). Although these correlations do not prove causation, they can guide insights in experimentally intractable systems, such as rockfishes. At a q -value cutoff of 0.05, we discovered 91 genes significantly associated with life span, including candidates with roles in cell growth and proliferation (e.g., *NRG1*), DNA repair (e.g., *BRCA1*), and suppression of apoptosis (e.g., *TNFRSF6B*) (Fig. 2D and fig. S9). However, life span in rockfishes is correlated with body size and environmental factors, such as depth (14). Thus, some of these genes associated with life span may act by influencing growth and size or may facilitate adaptations to environments that promote longevity.

To identify genes associated with rockfish longevity, independent of other factors, we constructed a linear model using the two most predictive variables for life span, size at maturity and maximum depth (Fig. 2E). This model described 59% of the variation in life span (Fig. 2F), which is comparable to simple models of life span and body size in mammals (15). Using the residuals of this model as

phenotypes, we identified 56 genes associated with life span independent of size at maturity or depth (Fig. 2D and table S14). These genes were overrepresented for insulin and glucose signaling (hypergeometric test, $P = 1.8 \times 10^{-6}$) (Fig. 2G and fig. S10), including genes with roles in life-span extension across many organisms (5). The rate of evolution for most of these genes was negatively correlated with life span, emphasizing the importance of nutrient-sensing maintenance in long-lived species. We also identified genes associated with reproductive aging in mice (16), the antiviral innate immunity factor *TRAF3IP3* (17), and the tumor suppressor *DYRK2* (18).

Of the 91 genes associated with life span, before correcting for size and depth, only 10 overlapped with those identified as associated with the life-span residual, suggesting that the majority ($n = 81$) of the genes we identified in *Sebastodes* act indirectly by influencing size or facilitating adaptations to depth. To parse the axes along which these life span-associated genes act, we correlated their relative evolutionary rates with either the growth-associated component of life span in our linear model (S , size), the depth-associated component of life span (D), or the residual of the model (R) (Fig. 2H). The size axis was associated with the most genes ($n = 33, S > 0.5$) in comparison to depth or the residual ($n = 18, D > 0.5; n = 17, R > 0.5$), which is in line with the importance of growth- and size-related pathways underlying differences in life span among different organisms (19). Pathways enriched along this axis included mTOR signaling DNA and telomere maintenance, and cancer (Fig. 2I). Genes and pathways along the D axis reflect environmental adaptations such as lipid metabolism and synthesis. The R axis was enriched for insulin signaling and protein homeostasis, with ribosome assembly pathways along the DR axis. Apoptosis genes were more closely clustered with the R axis intermediate to S and D , and antigen processing and presentation genes were also clustered along the SD axis. Together, these results suggest that the genetic basis of longevity in rockfish species may be due to the combined effect of genes acting directly on life span alongside genes affecting ecological and growth phenotypes that pleiotropically influence life span.

Expansion of the immune modulatory butyrophilin gene family in long-lived species

Gene duplications and structural rearrangements can drive evolutionary innovations (20, 21). To identify copy number changes associated with variation in life span, we performed a genome-wide screen using windowed read-depth-based copy estimates across chromosomes. Controlling for phylogenetic signal, we found an enrichment for positive associations between life span and copy number,

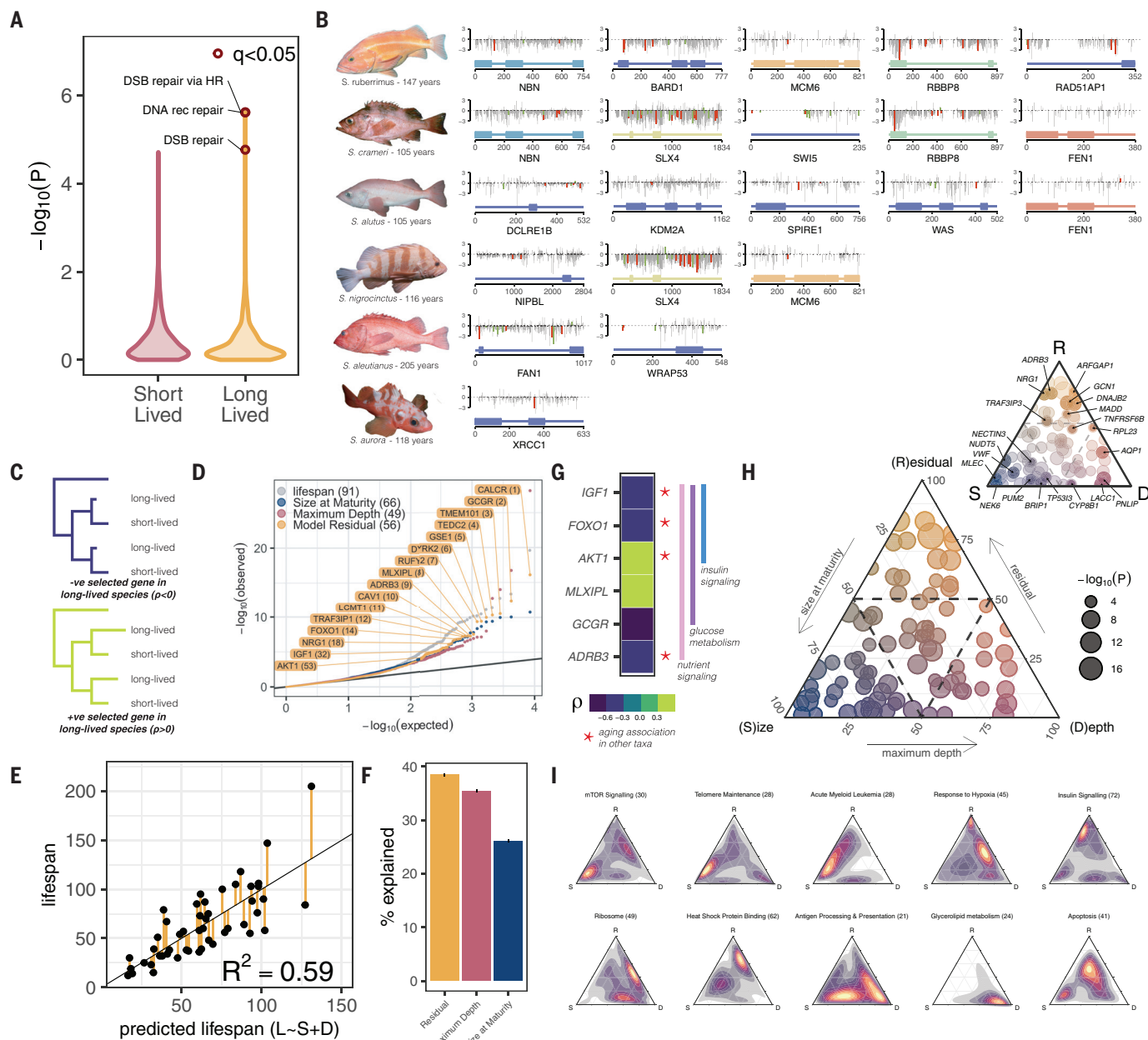


Fig. 2. Genetic underpinnings of life-span adaptations. (A) Distribution of pathway enrichment P values for genes under positive selection in short- and long-lived species. DSB, double-strand break; HR, homologous recombination; rec, recombination. (B) Schematics of the 16 DNA replication, repair, or maintenance genes exhibiting positive selection in long-lived rockfishes. Domain structure (bottom), gray lines indicate putative functional consequence of rockfish amino acid compared with human (PROVEAN score). Red and green bars indicate mutations distinct from all non-long-lived taxa colored by SIFT score – tolerated (green) / damaging (red). (C) Schematic representation of relative evolutionary rate test and (D) P value distribution of genes from relative evolutionary rate test (RERconverge) of correlation between evolutionary rate and individual traits. Life span and the individual components of a predictive linear model of

regardless of whether we used a short- or long-lived species reference (χ^2 , $P < 1 \times 10^{-15}$). The greatest cluster of positive associations was on chromosome 1 (Fig. 3A); it extended for almost 250 kb and overlapped nine genes (Fig. 3B)

ranging from zero to seven copies among different species (Fig. 3C). These nine genes included six members of the butyrophilin gene family (*BTN* and *BTNL* genes) (Fig. 3D), a family of immune regulators associated with

life span (E) are used as traits. Gene names are highlighted for the top 12 genes associated with the linear model residual as a trait in addition to four other significant gene candidates previously associated with aging (full gene list in table S14). (E) Linear regression model between maximum life span and predicted life span based on body size and depth for different species. (F) Proportion of variation in life span explained by size, depth, and the residual from the linear model. (G) Relative evolutionary rates of six genes involved in glucose, insulin, and nutrient signaling, four of which have been associated with aging in other taxa (table S14). (H) Ternary plot of 91 life span–associated genes plotted as a function of the relative importance along linear model axes, with dashed line at 50% (inset with gene labels) and (I) heatmaps of pathway enrichment along axes.

human inflammatory diseases (22). Using our linear model, we found that this signature is primarily driven by the depth-associated component of life span (Fig. 2H and fig. S15). Mutations in *BTNL2* cause sarcoidosis in humans

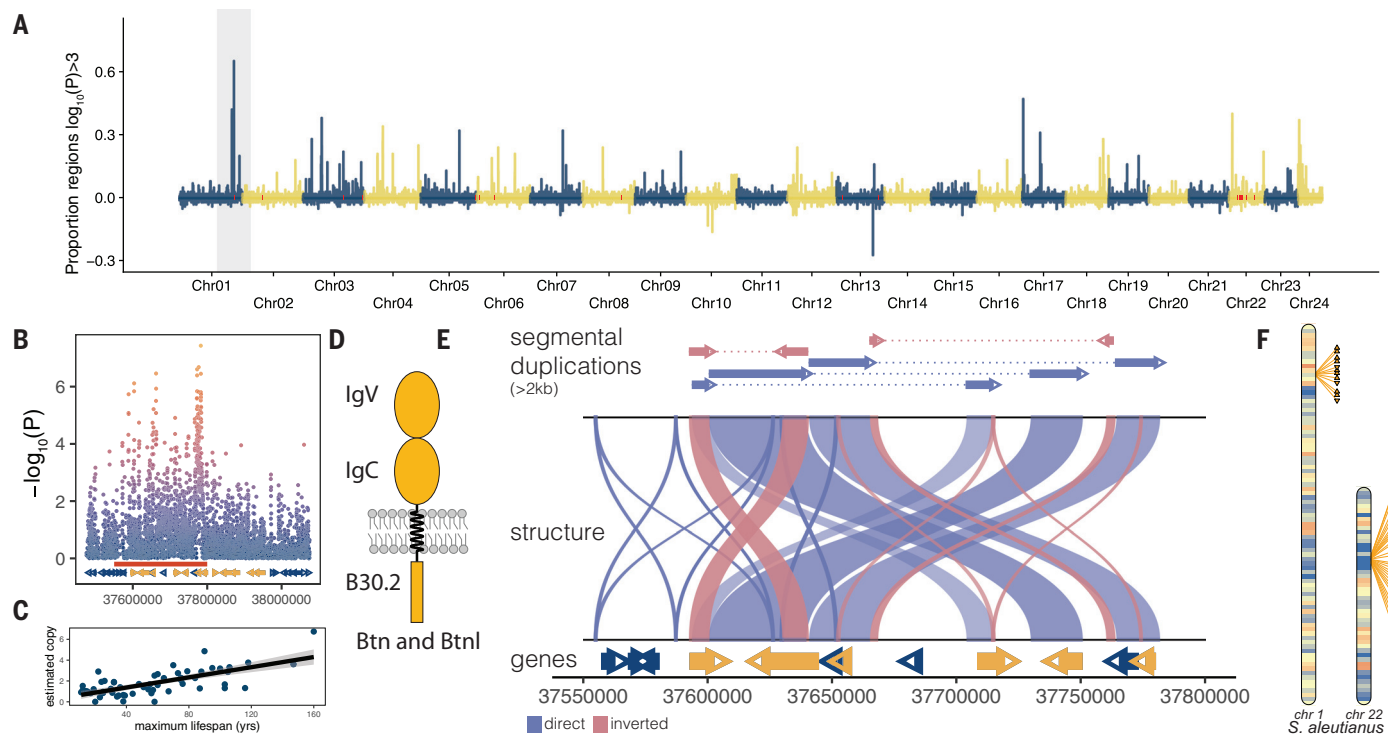


Fig. 3. Life span-associated butyrophilin gene duplications. (A) Miami plot of proportion of 100-bp regions with significant phylogenetic least squares linear model (PGLS) correlations between read-depth inferred copy number and life span (10-kb windows) across the *S. aleutianus* reference genome. (B) Manhattan plot of ~250-kb chromosome 1 butyrophilin locus and (C) copy number association. Butyrophilin genes shown in orange. (D) Protein structural organization of *BTN* and

BTNL gene family members. IgV, immunoglobulin V domain; IgC, immunoglobulin C domain. (E) Genome structure of the butyrophilin locus in the *S. aleutianus* genome assembly. Segmental duplications are highlighted above a self-alignment of the locus to show the underlying duplication architecture with genes below. (F) Karyotypes of chromosomes 1 and 22 in *S. aleutianus* (color indicates gene density) highlighting the two butyrophilin gene family clusters in *Sebastes* species.

(23), and variants in *BTN3A2* have been associated with human life span (24).

Butyrophilins are members of the B7 immunoglobulin superfamily and in response to inflammatory stimuli inhibit cytokine secretion and production in T cells, thus serving an immunosuppressive function. We resolved the underlying segmental duplication (SD) architecture of the life span-associated butyrophilin duplication in the *S. aleutianus* genome (Fig. 3E), identifying 22 large (>1 kb, >90% identity) SD blocks across the locus. The majority of the locus is contained in three pairs of large adjacent SDs in direct orientation, which together encompass 163 kb. Two large, high-identity (>95%) inverted duplications add additional complexity to the locus. While the copy number of *BTN* and *BTNL* genes at this locus correlates significantly (Fig. 3C) with life span in rockfishes, we identified *BTN* and *BTNL* copies not associated with life span as well, largely localized to two clusters on chromosomes 1 and 22 (Fig. 3F). Among our six *Sebastes* reference genome assemblies, the total number of *BTN* and *BTNL* genes ranges from 18 to 36, highlighting expansion of this gene family across taxa. Teleost fishes exhibit diverse immune

defense strategies, and gene expansions of the major histocompatibility complex I locus have occurred numerous times (25). Here, a distinct class of immunoregulatory genes in rockfishes may have facilitated adaptations to extreme life span.

Life-history transitions are tightly coupled to patterns of genetic diversity

To assess genetic diversity across the *Sebastes* clade, we performed variant calling on samples mapped to each of their respective genome assemblies. We identified a >13-fold range in heterozygosity among *Sebastes* species ($\pi = 2.9 \times 10^{-4}$ to 3.8×10^{-3} per base pair) (Fig. 4A) and a 20-fold range when the outgroup taxa were also considered. These levels of diversity correspond to a range in effective population size (N_e) of 7.2×10^4 to 9.6×10^5 in the *Sebastes* clade, assuming a mutation rate of 1×10^{-9} .

We applied multiple sequentially Markovian coalescent (MSMC) analysis (26) to dissect the demographic histories underlying these differences. We grouped MSMC trajectories by life-span quartile and compared the mean N_e over the last 10^6 generations (Fig. 4B). While we observed a wide range of dif-

ferent demographic trajectories, short-lived species exhibited increases in N_e over the past $\sim 10^6$ generations. Note that the short-lived African killifish exhibits reduced life span linked to severe population bottlenecks (27). However, rockfish life span was significantly negatively correlated with N_e as a function of maximum life span [phylogenetic generalized least squares (PGLS) $P = 0.005$] (Fig. 4C).

Body mass is strongly positively correlated with both census population sizes and life spans across terrestrial vertebrates (28, 29). In rockfishes too, size is correlated with life span (Fig. 2E), and, indeed, size is a better predictor of N_e than life span (PGLS $P = 6.6 \times 10^{-5}$) (Fig. 4D). These results suggest that life-history transitions to shortened life and smaller body size are potentially adaptive, in contrast to the drift-driven transitions observed in killifish. These results also underscore the inherent genetic vulnerability of larger long-lived marine fish species, which are often the targets of commercial fisheries (30).

Shifts in life span reshape the mutational spectrum of segregating genetic variation

Long-lived, larger, terrestrial vertebrates with smaller N_e often exhibit low rates of fecundity,

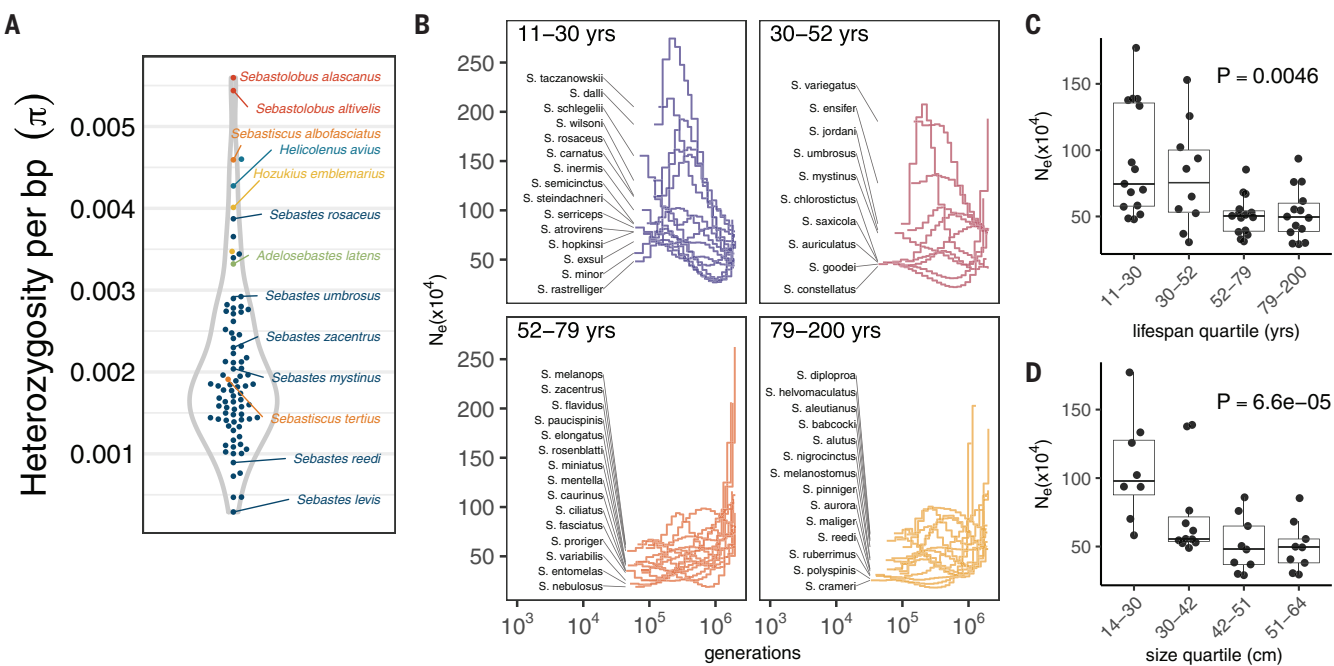
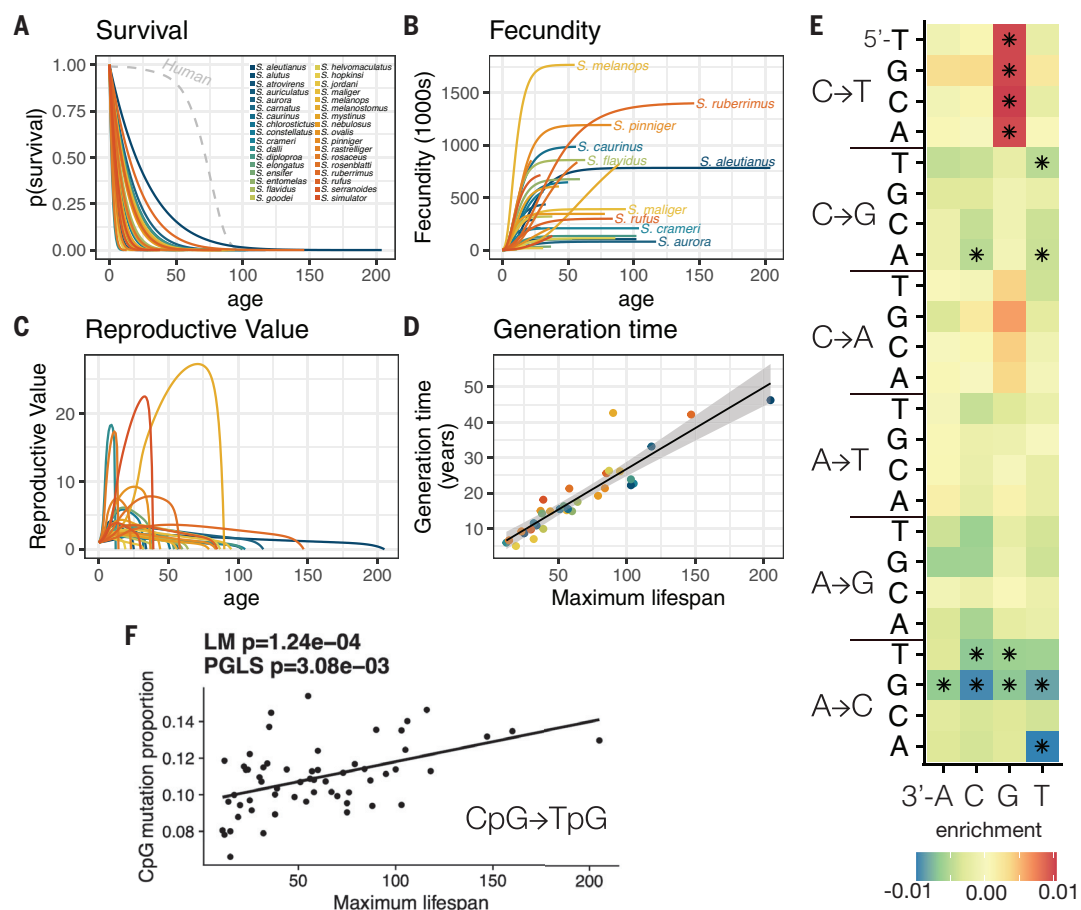


Fig. 4. Life-history transitions are associated with patterns of diversity. (A) Nucleotide diversity across 88 different species. (B) MSMC-based estimates of effective population sizes grouped by life span quartile over the last $\sim 10^6$ generations and averaged N_e grouped by (C) life-span quartile or (D) grouped by size quartile. Box and whisker plots indicate the median and interquartile range (IQR) with tails at the minimum and maximum values within $1.5 \times$ IQR. P values from PGLS linear model.

Fig. 5. Shifts in life-history traits reshape the mutational spectrum of segregating genetic variation. (A) Survival curves for 34 rockfish species. Humans, shown for comparison, exhibit maximum life spans similar to those of many rockfish species but different survival curves (type I versus type III survival). (B) Rockfish fecundity (births per season) plotted as a function of age. (C) Reproductive value plotted as a function of age. (D) Generation times estimated from survival and fecundity plotted as a function of life span. (E) Association of segregating single-nucleotide variant mutation types with life span across all trinucleotide contexts. Asterisks indicate age-associated mutational profiles significant after multiple testing correction ($q < 0.05$). (F) The proportion of segregating CpG \rightarrow TpG mutations as a function of maximum life span. LM, linear regression model.



increased maturation times, and higher survival of offspring (31). Long-lived rockfish species also exhibit extremely long maturation times stretching to more than a decade (3). We modeled survival, maturation, and fecundity in 34 different rockfish species for which detailed information could be ascertained to understand the evolutionary trade-offs driving rockfish life histories (Fig. 5, A to D, and tables S15 to S17). Similar to other marine fishes, rockfishes exhibit a “type III” survivorship curve, with high mortality at young ages and very few individuals surviving to old age (32) (Fig. 5A). However, fecundity increases rapidly as a function of age, proportional to size (Fig. 5B), and thus aging imparts minimal declines in their reproductive values (Fig. 5C). In extreme cases, such as in yelloweye rockfish (*S. ruberrimus*), 150-year-old individuals can produce more than one million offspring per season. Even compared with other marine fishes, which exhibit nonlinear scaling in reproductive output with size (33), older, larger rockfish have significantly higher reproductive output per unit weight (Wilcoxon $P = 6.3 \times 10^{-6}$) (fig. S20).

The disproportionate reproductive output of older fish results in generation times that span from 5 to 45 years across different species (Fig. 5D and table S17). We find that these differences in generation time and life span are associated with reduced nucleotide substitution rates (resulting in shortened phylogenetic branch lengths) in longer-lived species, as observed in terrestrial mammals (fig. S21) (34). Generation time can also influence the mutational spectrum, with certain classes of mutations being more likely to occur in older parents (35, 36). We thus classified species-specific segregating single-nucleotide variants by mutation type and trinucleotide context (fig. S22). Correlations between mutation types and life span (Fig. 5E) were seen with enrichments of CpG → TpG mutations; longer-lived species exhibited a significantly increased proportion of CpG transitions in all *CG → *TG contexts (PGLS $P = 1 \times 10^{-4}$) (Fig. 5F). CpG → TpG transitions are characteristic of spontaneous methylated cytosine deamination, a mutational signature that occurs independent of DNA replication (37) and is the dominant age-associated mutational profile of human tumors (38).

In humans, a reduced proportion of CpG variants in European populations has been hypothesized to have been driven by shortened generation times (39), which, if due to similar processes in fish, may be consistent with our findings. A number of mutational signatures were also at reduced frequency across long-lived rockfish species, including A → C and C → G transversions (Fig. 5E), however it is unclear what the underlying mutational mechanism of this signature might be.

Together, these results indicate that shifts in life histories can in turn reshape patterns of segregating genetic diversity.

Discussion

The vast diversity of life histories in Pacific Ocean rockfishes presents an opportunity to dissect the genetic adaptations that shape life-history transitions in vertebrates. Our results highlight selective signatures in pathways underlying “hallmarks of aging” (4) that are conserved across all eukaryotes (e.g., DNA damage and nutrient-sensing pathways) as well as in vertebrate-specific hallmarks such as immunity and inflammation (5). Chronic inflammation (“inflammaging”) in particular has emerged as a key therapeutic target in humans, and our results identify a specific gene family, the butyrophilins, that may play a role in modulating life span in rockfishes. We also find that the genetic adaptations that enable extreme longevity in rockfishes do so both directly, by influencing insulin signaling and other key pathways, as well as indirectly, by influencing size and adaptations to depth. Further, our results indicate that such life-history transitions themselves reshape patterns of genetic diversity. Long-lived rockfish species exhibit reduced genetic diversity in contrast to short-lived species, and the mutational spectrum of segregating genetic variation is also altered by life span. Indeed, the disproportionately higher reproductive output in older, larger rockfishes is likely directly linked to their extreme longevity. Our work further highlights the utility of genus-wide genome assembly efforts to answer questions that have thus far been limited to representative species from broad taxonomic groups (e.g., vertebrates). The advent of additional complete genome assemblies from vertebrates will advance our understanding of the generality of our findings across evolutionary and physical scales.

REFERENCES AND NOTES

- B. Charlesworth, *Genetics* **156**, 927–931 (2000).
- M. Depczynski, D. R. Bellwood, *Curr. Biol.* **15**, R288–R289 (2005).
- J. Nielsen et al., *Science* **353**, 702–704 (2016).
- C. López-Otin, M. A. Blasco, L. Partridge, M. Serrano, G. Kroemer, *Cell* **153**, 1194–1217 (2013).
- P. P. Singh, B. A. Demmitt, R. D. Nath, A. Brunet, *Cell* **177**, 200–220 (2019).
- M. S. Love, M. Yoklavich, L. Thorsteinson, *The Rockfishes of the Northeast Pacific* (Univ. of California Press, ed. 1, 2002).
- D. L. Rabosky et al., *Nature* **559**, 392–395 (2018).
- M. Seppey, M. Manni, E. M. Zdobnov, in *Gene Prediction: Methods and Protocols*, M. Kollmar, Ed. (Methods in Molecular Biology, Springer, 2019), pp. 227–245.
- Materials and methods are available as supplementary materials.
- J. R. Hyde, R. D. Vetter, *Mol. Phylogenet. Evol.* **44**, 790–811 (2007).
- M. Keane et al., *Cell Rep.* **10**, 112–122 (2015).
- V. Quesada et al., *Nat. Ecol. Evol.* **3**, 87–95 (2019).
- A. Kowalczyk et al., *Bioinformatics* **35**, 4815–4817 (2019).
- M. Mangel, H. K. Kindsvater, M. B. Bonsall, *Evolution* **61**, 1208–1224 (2007).
- S. N. Austad, K. E. Fischer, *J. Gerontol.* **46**, B47–B53 (1991).
- T. Umehara et al., *Aging Cell* **16**, 1288–1299 (2017).
- M. Deng et al., *Nat. Commun.* **11**, 2193 (2020).
- V. Tandon, L. de la Vega, S. Banerjee, *J. Biol. Chem.* **296**, 100233 (2021).
- D. E. Promislow, *J. Gerontol.* **48**, B115–B123 (1993).
- M. Todesco et al., *Nature* **584**, 602–607 (2020).
- P. H. Sudmant et al., *Science* **349**, aab3761 (2015).
- H. A. Arnett, J. L. Viney, *Nat. Rev. Immunol.* **14**, 559–569 (2014).
- R. Valençente et al., *Nat. Genet.* **37**, 357–364 (2005).
- K. M. Wright et al., *G3* **9**, 2863–2878 (2019).
- M. Malmstrom et al., *Nat. Genet.* **48**, 1204–1210 (2016).
- S. Schiffels, R. Durbin, *Nat. Genet.* **46**, 919–925 (2014).
- R. Cui et al., *Cell* **178**, 385–399.e20 (2019).
- S. I. Nikolaev et al., *Proc. Natl. Acad. Sci. U.S.A.* **104**, 20443–20448 (2007).
- K. Popadin, L. V. Polishchuk, L. Mamirova, D. Knorre, K. Gunbin, *Proc. Natl. Acad. Sci. U.S.A.* **104**, 13390–13395 (2007).
- J. Rolland, D. Schlüter, J. Romiguier, *Mol. Biol. Evol.* **37**, 2192–2196 (2020).
- E. R. Pianka, *Am. Nat.* **104**, 592–597 (1970).
- E. S. Deevey Jr., *Q. Rev. Biol.* **22**, 283–314 (1947).
- D. R. Barneche, D. R. Robertson, C. R. White, D. J. Marshall, *Science* **360**, 642–645 (2018).
- M. A. W. Sayres, C. Venditti, M. Pagel, K. D. Makova, *Evolution* **65**, 2800–2815 (2011).
- A. P. Martin, S. R. Palumbi, *Proc. Natl. Acad. Sci. U.S.A.* **90**, 4087–4091 (1993).
- H. Jónsson et al., *Nature* **549**, 519–522 (2017).
- L. Séguirel, M. J. Wyman, M. Przeworski, *Annu. Rev. Genomics Hum. Genet.* **15**, 47–70 (2014).
- J. G. Tate et al., *Nucleic Acids Res.* **47**, D941–D947 (2019).
- K. Harris, J. K. Pritchard, *eLife* **6**, e24284 (2017).
- G. Owens, R. Kolora, P. Sudmant, sudmantlab/rockfishgenomoproject: RGP_codebase_v1.3, version 1.3, Zenodo (2021); <https://doi.org/10.5281/zenodo.5535007>.

ACKNOWLEDGMENTS

We acknowledge L. Smith and A. Bentley of the University of Kansas Biodiversity Institute and M. Miya at Chiba Natural History Museum and Institute for their assistance in sample acquisition. We thank the National Oceanic and Atmospheric Administration’s Alaska Fisheries Science Center, RACE Division, for specimens collected during resource assessment surveys. Fish image credits: Kyoto University, Fish Collection; SWFSC ROV Team; R. R. Lauth, Alaska Fisheries Science Center; D. E. Stevenson, Alaska Fisheries Science Center; J.W.O.; J. Nichols; C. Grossmann; D. Karimoto; P. Ridings; K. Lee; M. Chamberlain; M. Guimaraes; and S. Geiter. We also thank M. Slatkin for helpful discussions. **Funding:** National Institute of General Medical Sciences grant R35GM142916 to P.H.S.

Author contributions: P.H.S. conceptualized and designed the experiment. A.S., C.J., K.S., J.A.V., K.M., M.M., M.W.S., J.W.O., and M.L. coordinated sample collection efforts. S.R.R.K., G.L.O., J.M.V., and P.H.S. performed all analyses. K.C. and D.B. performed Hi-C experiments for genome assembly. P.H.S., G.L.O., S.R.R.K., and M.L. wrote the manuscript. **Competing interests:** The authors declare no competing interests. **Data and materials availability:** All sequencing data have been deposited in the European Nucleotide Archive under accession PRJEB42258. Complete methods are described in the supplementary materials (9), and all code required to recapitulate analyses, including BUSCO gene alignments and gene trees, has been posted at Zenodo (40).

SUPPLEMENTARY MATERIALS

- science.org/doi/10.1126/science.abg5332
 - Materials and Methods
 - Figs. S1 to S23
 - Tables S1 to S17
 - References (41–84)
 - MDAR Reproducibility Checklist
 - [View/request a protocol for this paper from Bio-protocol.](https://bio-protocol.org)
- 12 November 2021; resubmitted 27 May 2021
Accepted 7 October 2021
10.1126/science.abg5332

Origins and evolution of extreme life span in Pacific Ocean rockfishes

Sree Rohit Raj Kolora¹ Gregory L. Owens² Juan Manuel Vazquez³ Alexander Stubbs⁴ Kamalakar Chatla⁵ Conner Jainese⁶ Katelin Seeto⁷ Merit McCrea⁸ Michael W. Sandel⁹ Juliana A. Vianna¹⁰ Katherine Maslenikov¹¹ Doris Bachtrog¹² James W. Orr¹³ Milton Love¹⁴ Peter H. Sudmant¹⁵

Science, 374 (6569), • DOI: 10.1126/science.abg5332

A fishy tale of long and short life span

Fish have wide variations in life span even within closely related species. One such example are the rockfish species found along North Pacific coasts, which have life spans ranging from 11 to more than 200 years. Kolora *et al.* sequenced and performed a genomic analysis of 88 rockfish species, including long-read sequencing of the genomes of six species (see the Perspective by Lu *et al.*). From this analysis, the authors unmasked the genetic drivers of longevity evolution, including immunity and DNA repair–related pathways. Copy number expansion in the butyrophilin gene family was shown to be positively associated with life span, and population historical dynamics and life histories correlated differently between long- and short-lived species. These results support the idea that inflammation may modulate the aging process in these fish. —LMZ

View the article online

<https://www.science.org/doi/10.1126/science.abg5332>

Permissions

<https://www.science.org/help/reprints-and-permissions>